Journal of Magnetism and Magnetic Materials 422 (2017) 43–48

Contents lists available at ScienceDirect

Journal of Magnetism and Magnetic Materials

journal homepage: www.elsevier.com/locate/jmmm

Mechanochemical synthesis of magnetically hard anisotropic $RFe_{10}Si_2$ powders with R representing combinations of Sm, Ce and Zr

A.M. Gabay *, G.C. Hadjipanayis

Department of Physics and Astronomy, University of Delaware, 217 Sharp Lab, Newark, DE 19716, USA

ARTICLE INFO

Article history:
Received 29 January 2016
Received in revised form
7 August 2016
Accepted 21 August 2016
Available online 22 August 2016

Keywords:
Permanent magnet
Rare earth-lean magnet
ThMn12
Mechanochemistry
Coercivity

ABSTRACT

Alloy synthesis consisting of mechanical activation followed by annealing was explored as a method of manufacturing medium-grade permanent magnet materials with a reduced content of the critical rare earth elements. Four $R_xFe_{10}Si_2$ alloys with R=Sm, $Sm_{0.7}Zr_{0.3}$, $Sm_{0.3}Ce_{0.3}Zr_{0.4}$ and $Ce_{0.6}Zr_{0.4}$ (nominal compositions) were prepared from mixtures of Sm_2O_3, CeO_2, ZrO_2, Fe_2O_3 and Si powders in the presence of a reducing agent Ca and a CaO dispersant. The collected alloy particles typically consisted of few joined submicron crystals. For R=Sm, X-ray diffraction analysis reveals a significant amount of the unwanted Th_2Zn_{17}-type compound forming alongside the desired $ThMn_{12}$-type 1:12 compound. A more pure 1:12 phase could be obtained for R=$Ce_{0.6}Zr_{0.4}$, but it exhibited a room-temperature coercivity of less than 1 kOe. The most pure 1:12 phase and the highest values of the coercivity (10.8 kOe) and calculated maximum energy product (13.8 MGOe) were obtained for R=$Sm_{0.7}Zr_{0.3}$ processed at 1150 °C. The calculated maximum energy products of the $Sm_{0.3}Ce_{0.3}Zr_{0.4}Fe_{10}Si_2$ particles, with half of their rare earths constituents represented by the relatively abundant Ce, was 10.1 MGOe.

1. Introduction

In the wake of the 2010–11 rare earths (REs) supply crisis there currently exists a strong incentive to reduce the dependence of energy-dense permanent magnets on the RE elements [1]. Although the development of RE-*free* magnets which would exhibit a maximum energy product $(BH)_{max}$ of at least 12–15 MGOe greatly intensified in recent years, the advancement towards that goal has been slow. The RE-Fe alloys based on the $ThMn_{12}$-type crystal structure may offer a compromise solution – iron-based magnets containing *less* REs and none of the high-demand REs involved in manufacturing of the Nd-Fe-B magnets. These application prospects must be among the reasons behind the renewed interest in the $Sm(Fe,M)_{12}$ [2,3] and the isotypical compounds with Ce [4–9]. Moreover, in the case of M=Si, the concentration of the (light) RE element can be further reduced by substituting this element with Zr [10–12].

Apart from the $Nd(Fe,M)_{12}N_x$ nitrides, which are less interesting in this context because of their dependence on Nd and structural instability, the 1:12 compounds with the highest hard magnetic potential are $Sm(Fe,M)_{12}$ [13]. Indeed, the room-temperature intrinsic coercivities H_c of 11–12 kOe have been achieved in $Sm(Fe,Ti,V)_{12}$ [14–16]. However, these H_c values – unexceptional for compounds characterized by an anisotropy field H_a close to 100 kOe [17] – could only be obtained in isotropic nanocrystalline materials prepared via melt-spinning or mechanical alloying. Impossibility to align the easy magnetization directions of the crystallites in such materials dramatically lowers their achievable $(BH)_{max}$. One factor unfavorable for the development of a high H_c in the $Sm(Fe,M)_{12}$ compounds is that at equilibrium they coexist with soft magnetic phases [13]. Another powerful impediment is the typically high formation temperatures of the 1:12 structure [18]. The difficulty to combine the high-temperature treatment with the nanostructure needed for a high H_c can explain the low H_c values reported for the alloys based on $SmFe_{10}Si_2$ and $Sm_{0.7}Zr_{0.3}Fe_{10}Si_2$ (only 4 kOe [19] and 3.2 kOe [11], respectively) despite the high $H_a \approx 120$ kOe of the former compound [17].

The mechanochemical synthesis (a reduction-diffusion of mechanically activated precursors) of high-H_a compounds has been shown [20] not only to produce H_c values comparable to those in nanocrystalline materials, but also to yield *anisotropic*, often single crystal particles with the theoretical $(BH)_{max}$ approaching that of the compound. Indeed, a superior $(BH)_{max}$ value was recently obtained in submicron $Sm(Fe,Co,Ti)_{12}$ particles prepared this way [21]. Somewhat larger $Nd(Fe,Mo)_{12}$ particles prepared via reduction-diffusion of *chemically* synthesized precursors showed a noticeable H_c after subsequent nitrogenization [22]. Importantly, the (removable) byproducts of the reduction as well as the often-added (removable) dispersant may not only keep the synthesized particle apart, but also restrict their growth, thus mitigating the

* Corresponding author.
E-mail address: gabay@udel.edu (A.M. Gabay).

http://dx.doi.org/10.1016/j.jmmm.2016.08.064
0304-8853/

detrimental effect of a high synthesis temperature on the H_c. One noteworthy aspect of the synthesis of tetragonal $R(Fe,M)_{12}$ structures, is that they may be seen as the result of ordering in the respective $TbCu_7$-type hexagonal structures [23]; such ordering transformations were observed experimentally [24]. Besides the tetragonal $ThMn_2$-type structures, ordering in the Fe-rich R(Zr)-Fe-Si alloys with the $TbCu_7$-type structure (which are characterized by broad ranges of the compositions) are known to produce the rhombohedral structures of the Th_2Zn_{17} type [25,26], the hexagonal structures of the Th_2Ni_{17} type [12] and the monoclinic structures of the $Nd_3(Fe,Ti)_{29}$ type [27].

In this paper, we report the mechanochemical synthesis and subsequent characterization of several $RFe_{10}Si_2$ compounds demonstrating that this preparation method in combination with a Zr substitution for the REs markedly improves their prospects as permanent magnet materials.

2. Experiment

The raw materials used in the synthesis were powders of Sm_2O_3 (particles ≤ 1 μm, nominal purity 99.9%), CeO_2 (≤ 1 μm, 99.9%), ZrO_2 (≤ 2 μm, 99%), Fe_2O_3 (≤ 0.5 μm, 99%) and crystalline Si (≤ 45 μm, 99.999%), 1 mm granules of 99.5% Ca metal and 0.5–1.0 μm CaO particles (the dispersant) prepared by firing a submicron $CaCO_3$ powder (98%) at 900 °C. The amounts of the reactants corresponded to the mole ratios between the three R elements (Sm, Ce and Zr) and – separately – between Fe and Si as in the four "target" $RFe_{10}Si_2$ compositions: $SmFe_{10}Si_2$, $Sm_{0.7}Zr_{0.3}Fe_{10}Si_2$, $Sm_{0.3}Ce_{0.3}Zr_{0.4}Fe_{10}Si_2$ and $Ce_{0.6}Zr_{0.4}Fe_{10}Si_2$. Significant excesses of the R elements and the metallic Ca were required to obtain the 1:12 structures; the used (Fe+Si)/R and Ca/O ratios are listed in Table 1. The mass of the added CaO dispersant was 3 times the mass of the reactants other than the metallic Ca. Hereafter we refer to the samples resulted from the four mixtures via the R component(s): Sm, $Sm_{0.7}Zr_{0.3}$, $Sm_{0.3}Ce_{0.3}Zr_{0.4}$ and $Ce_{0.6}Zr_{0.4}$. After a thorough mixing, the precursors were mechanically activated by milling for 4 h in argon with steel balls (six 12 mm balls for 5 g of the mixture) using a Spex-8000 high-energy mill. The subsequent annealing at temperatures T_a varying from 850 to 1200 °C was done – without exposing the activated powders to the air – in argon-filled quartz capsules placed in the preheated furnace for 5 min (unless other time is specified; selected samples were annealed for up to 1200 min). The powders were protected from reacting with the quartz by open-ended reusable Mo-foil cartridges.

In order to collect the synthesized ferromagnetic particles, 0.3 g of the annealed mixture was sequentially washed in 40 ml of 25 vol% glycerol (3 × 7 min), deionized water (2 × 1 min), 0.1 vol% acetic acid (1 min), again water (1 min) and, finally, ethanol (2 × 1 min). The washing was performed under ultrasound irradiation (a Sonics & Materials VCX750 ultrasound generator) in an ice-water bath; each of the nine steps was followed by magnetic separation of the products. At the end, the collected particles were dried in air in a magnetic field.

The materials were characterized with X-ray diffraction (XRD; a Rigaku Ultima IV instrument; the Cu Kα radiation), scanning electron microscopy (SEM; a JEOL JSM-6335F instrument) and energy-dispersive spectroscopy (EDS, an IXRF Systems instrument). The XRD results were analyzed with the Powder Cell software [28]. Powder samples for the magnetic characterization were immobilized with paraffin wax, some of them under a magnetic field. Room-temperature demagnetization curves were recorded with a Quantum Design VersaLab vibrating sample magnetometer (uncertainty ± 0.5 emu/g) after magnetizing the samples with a pulsed field of 100 kOe. Correction for self-demagnetization, when it is specified, was done with demagnetization factors determined for similarly prepared Fe powders.

Table 1
Mole ratios defining amounts of the reactants for synthesis of specific 1:12 compounds (not counting the added CaO dispersant).

Target composition	(Fe+Si)/(Sm+Ce+Zr)	Ca/O
$SmFe_{10}Si_2$	6.42	1.55
$Sm_{0.7}Zr_{0.3}Fe_{10}Si_2$	6.42	1.50
$Sm_{0.3}Ce_{0.3}Zr_{0.4}Fe_{10}Si_2$	6.85	1.50
$Ce_{0.6}Zr_{0.4}Fe_{10}Si_2$	6.81	1.50

3. Results

In the samples prepared with R=Sm and annealed for 5 min at progressively increasing T_a, the XRD peaks consistent with the tetragonal 1:12 structure were first detected for T_a=950 °C (Fig. 1; note that the principal phase in the as-annealed samples is CaO, which had been added as the dispersant and also forms as a by-product of the synthesis). This apparent emergence of the 1:12 phase was accompanied by an increase of the H_c from 0.4 to 2.0 kOe (Fig. 2). The $ThMn_{12}$-type $SmFe_{10}Si_2$ structure in *ingots* was obtained [29] through a much longer (10 days) annealing at 950 °C. The mechanochemical synthesis at this temperature for 1200 min produced – according to the XRD data shown in Fig. 1 – a 1:12 structure characterized by lattice parameters a=0.8480 (5) nm and c=0.4800(5) nm, but the (washed) sample also

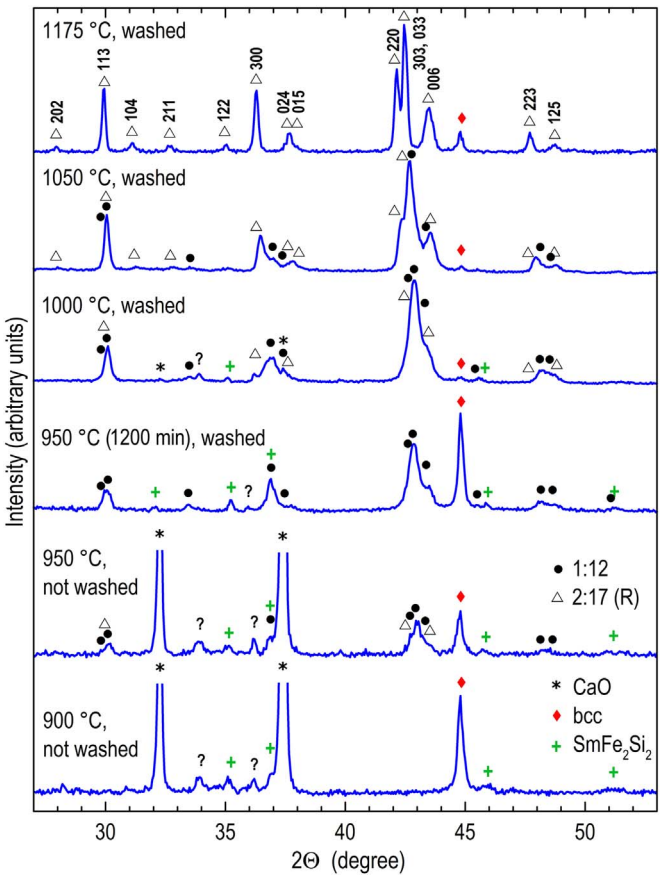

Fig. 1. XRD spectra of $R_xFe_{10}Si_2$ samples prepared with R=Sm for selected annealing temperatures T_a. The T_a and post-annealing treatment are indicated; when not specified, the annealing time was 5 min. "1:12" and "2:17R" stand for the $ThMn_{12}$ and Th_2Zn_{17} structure types, respectively.

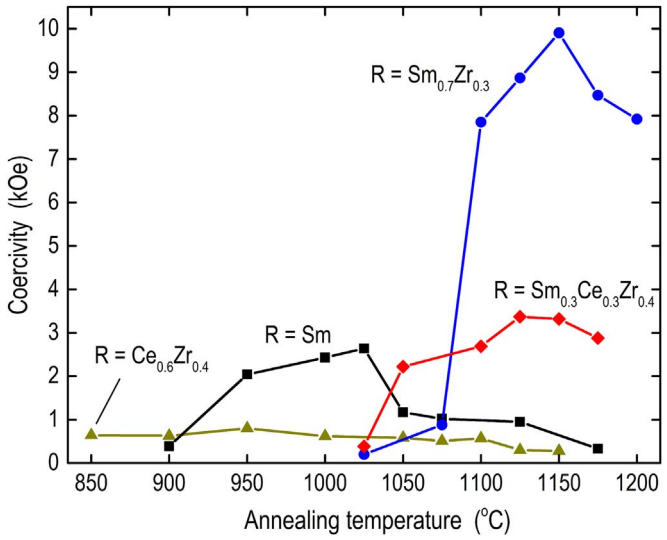

Fig. 2. Room-temperature coercivity of as-synthesized (not washed) $R_xFe_{10}Si_2$ samples as a function of annealing temperature T_a.

contained a significant amounts a bcc Fe-based solid solution and a phase identified as the tetragonal $SmFe_2Si_2$ [30]. The highest room-temperature H_c of the R=Sm alloys synthesized at T_a=950 °C for 5–1200 min was 2.8 kOe; this value was obtained after the annealing for 180 min.

In the R=Sm alloys annealed for 5 min at $T_a > 950$ °C, the 1:12 phase was found to be increasingly replaced by the rhombohedral Th_2Zn_{17}-type structure ("2:17R"), which is based on the same precursor structure of the $TbCu_7$ type. The room-temperature H_c increases with T_a reaching its maximum value of 2.6 kOe at T_a=1025 °C. This increase correlates with a decreasing amount of the magnetically soft bcc phase in the alloys dominated by the 1:12 phase. However, the lower-than-expected intensity of the (310) superstructure reflection of the 1:12 structure at $2\theta \approx 33.4°$ (see the XRD spectrum of the sample annealed at 1000 °C, Fig. 1) may indicate that this structure had been only *partially* ordered from the $TbCu_7$-type structure. Together with the presence of the magnetically soft 2:17R phase, this possible partial ordering, may explain the relatively low H_c as compared to the anisotropy field of the $SmFe_{10}Si_2$ compound. When the T_a is increased to 1050 °C, the 2:17R becomes the majority phase, and the H_c of the alloy falls to 1.2 kOe. Sample synthesized at 1175 °C is dominated by the 2:17R structure [a=0.8579(3) nm, c=1.2486(5) nm] with the bcc structure as the minority phase; the coercivity for this sample is only 0.3 kOe. Thus, neither a pure 1:12 structure nor an H_c exceeding 3 kOe could be obtained for R=Sm.

A very different crystallization sequence could be observed for R=$Sm_{0.7}Zr_{0.3}$. In this case, the XRD does not detect the 1:12 structure until T_a exceeds 1025 °C (see Fig. 3a). On the other hand, the 1:12 phase detected for 1075 °C ≤ T_a ≤ 1175 °C is the only *RE-Fe-based* phase identified in the sample. For T_a=1150 °C, when the XRD detects the smallest amount of the bcc phase (Fig. 3a), the 1:12 phase is nearly the only *magnetic* phase in the sample; for this T_a the room-temperature coercivity reaches its highest value of 9.9 kOe (Fig. 2). The R=$Sm_{0.3}Ce_{0.3}Zr_{0.4}$ sample behaves rather similarly, except that a small amount of the 1:12 phase can be seen already for T_a=1025 °C, and a $Zr_6Fe_{16}Si_7$ minority phase [the $Mg_6Cu_{16}Si_7$ type, a=1.1579(5) nm] forms for $T_a \geq 1050$ °C (see Fig. 3b). The highest H_c – again corresponding to the minimum amount of the bcc soft magnetic phase – is 3.4 kOe (Fig. 2). In the Sm-free samples with R=$Ce_{0.6}Zr_{0.4}$, both the 1:12 and $Zr_6Fe_{16}Si_7$ phases can be detected for T_a as low as 850 °C (see Fig. 3c). Like in the case of R=Sm, a second RE-Fe-based phase forms here besides the 1:12 phase, but for R=$Ce_{0.6}Zr_{0.4}$ it has the hexagonal Th_2Ni_{17}-type structure ("2:17H"). The effect of annealing temperature on the H_c of the materials prepared with R=$Ce_{0.6}Zr_{0.4}$ is weak compared to the other R components, and the H_c reaches only 0.8 kOe (Fig. 2).

In the three Zr-containing materials, the largest volume fraction of the 1:12 structure was observed for the samples processed at 1150 °C (see Fig. 3). The XRD data for a *washed* sample shown in Fig. 4a confirm the nearly pure 1:12 structure in the $Sm_{0.7}Zr_{0.3}Fe_{10}Si_2$ alloy containing only around 1 vol% of the bcc phase. The washed $Sm_{0.3}Ce_{0.3}Zr_{0.4}Fe_{10}Si_2$ alloy contains additionally some 7% of the $Zr_6Fe_{16}Si_7$ phase (Fig. 4b). The 1:12 structure is the least pure in the washed "$Ce_{0.6}Zr_{0.4}Fe_{10}Si_2$" alloy, where it co-exists with approximately 27% of the 2:17H and 8% of the $Zr_6Fe_{16}Si_7$ (Fig. 4c). A 0.3–0.4% expansion of the 1:12 unit cell was found to occur during the washing, most probably as a result of interstitial modification of the 1:12 lattice with hydrogen produced by reaction between the unreacted Ca and water [31]. Interestingly, the washed $Sm_{0.3}Ce_{0.3}Zr_{0.4}Fe_{10}Si_2$ alloy exhibited a 30% higher H_c than immediately after the synthesis; the corresponding figures as presented in Table 2. The typical particles which are shown in Fig. 5 are slightly smaller than 1 μm. Some of them appear to be single crystals, but most consist of a few joined crystals.

Fig. 6 presents the room-temperature demagnetization curves for the *oriented* $Sm_{0.7}Zr_{0.3}Fe_{10}Si_2$ and $Sm_{0.3}Ce_{0.3}Zr_{0.4}Fe_{10}Si_2$ powders featuring predominantly the 1:12 structure. Although the curves 1 and 2 measured parallel to the direction of the orienting field differ significantly from the curves 1′ and 2′ measured perpendicularly, they are not saturated as it would be if *all* the [001] easy magnetization directions were parallel to the applied field. The observed *partial* alignment is consistent with the number of the 1:12 crystallites in the typical alloy particles; although larger than one, this number is not large enough to ensure quasi-isotropic behavior of the particle. Still, the remanent magnetizations of the aligned $Sm_{0.7}Zr_{0.3}Fe_{10}Si_2$ and $Sm_{0.3}Ce_{0.3}Zr_{0.4}Fe_{10}Si_2$ powders, 89.0 and 87.2 emu/g respectively, are markedly higher than 45–65 emu/g reported for the nanocrystalline $Sm(Fe,M)_{12}$ alloys [9,14,15,19,32]. A rough estimate of the anisotropy field as the intersect of the extrapolated $M(H)$ curves (for two *unsaturated* curves such extrapolation may be unreliable) produces $H_a \approx 87$ kOe for the $Sm_{0.7}Zr_{0.3}Fe_{10}Si_2$ – which is close to 85 kOe reported in [11] – and ≈ 47 kOe for the $Sm_{0.3}Ce_{0.3}Zr_{0.4}Fe_{10}Si_2$. The H_c values of the two powders are roughly proportional to their respective H_a: 10.8 and 5.2 kOe. Thus, the coercivity of the mechanochemically synthesized anisotropic $Sm_{0.7}Zr_{0.3}Fe_{10}Si_2$ powder practically matches the highest values reported for the nanocrystalline $Sm(Fe,M)_{12}$ alloys [14–16]. Note that the alignment further increases the H_c of the $Sm_{0.3}Ce_{0.3}Zr_{0.4}Fe_{10}Si_2$ powder compared to the values listed in Table 2.

4. Discussion

The correlation between the presence of the 1:12 structure and the H_c is obvious for the three Sm-containing materials, but not in the case of R=$Ce_{0.6}Zr_{0.4}$. One possible explanation for the apparent inconsistency is the effect of the crystallite size. Although this size was not systematically monitored in the present work, its expected increase with the T_a should have adversely affected the H_c of all four studied materials. The coercivity of the $Ce_{0.6}Zr_{0.4}Fe_{10}Si_2$ particles may be especially sensitive to their size, because this alloy stands apart with its weakest magnetocrystalline anisotropy. The corresponding H_a was reported to be 24 kOe [12], half the value estimated for the $Sm_{0.3}Ce_{0.3}Zr_{0.4}Fe_{10}Si_2$ in this work.

The presented results may indicate that the partial Zr substitution for Sm in the $SmFe_{10}Si_2$ compound shifts the range of the

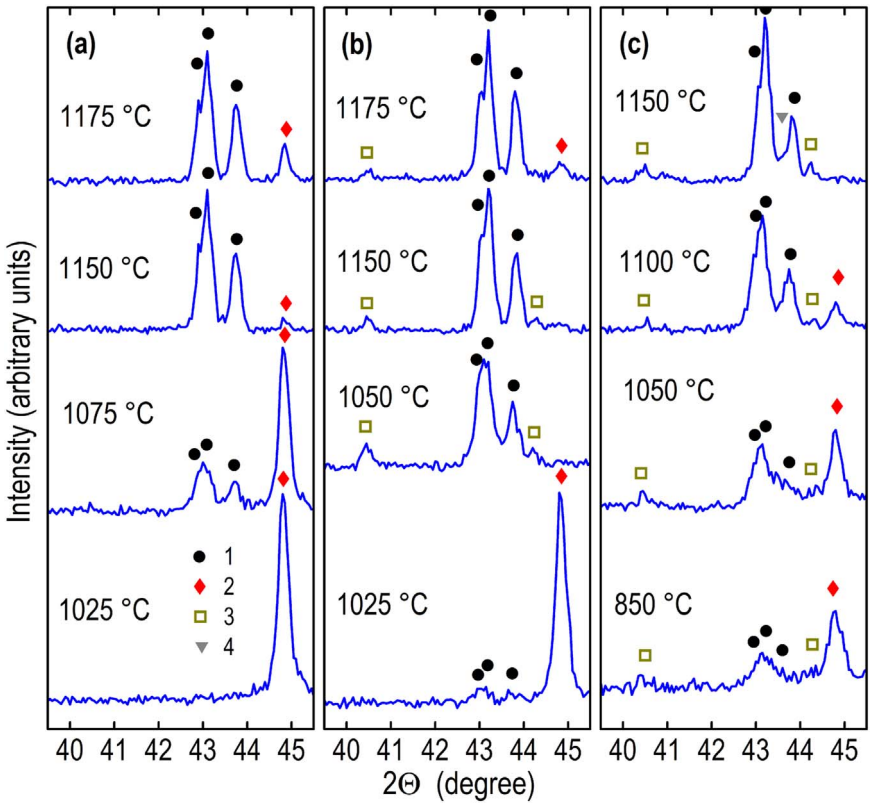

Fig. 3. XRD spectra of as-synthesized $R_xFe_{10}Si_2$ samples where R is (a) $Sm_{0.7}Zr_{0.3}$, (b) $Sm_{0.3}Ce_{0.3}Zr_{0.4}$, and (c) $Ce_{0.6}Zr_{0.4}$ for selected annealing temperatures T_a. Identified structures are: 1 – $ThMn_{12}$ type, 2 – bcc, 3 – $Zr_6Fe_{16}Si_7$, 4 – Th_2Ni_{17} type.

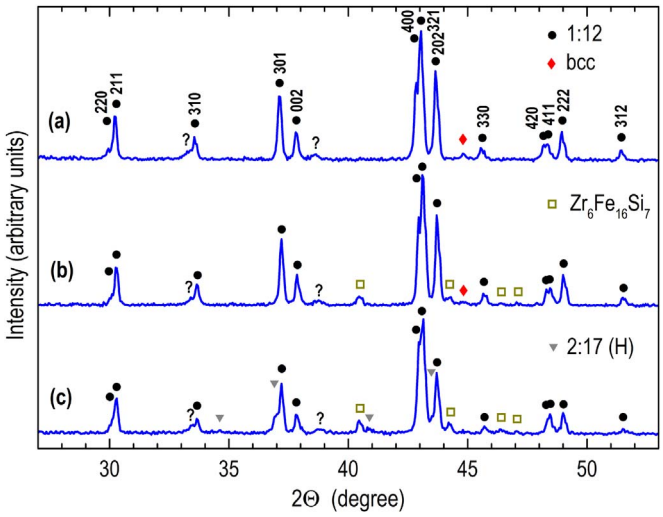

Fig. 4. XRD spectra of (a) $Sm_{0.7}Zr_{0.3}Fe_{10}Si_2$, (b) $Sm_{0.3}Ce_{0.3}Zr_{0.4}Fe_{10}Si_2$, and (c) $Ce_{0.6}Zr_{0.4}Fe_{10}Si_2$ powders collected (washed) after processing at $T_a = 1150$ °C. "1:12" and "2:17 H" stand for the $ThMn_{12}$ and Th_2Ni_{17} structure types, respectively.

Table 2
Lattice parameters and unit cell volume of the 1:12 structure and coercivity values determined for samples prepared with $R = Sm_{0.3}Ce_{0.3}Zr_{0.4}$ and processed at $T_a = 1150$ °C.

	As-synthesized	Washed
a (nm)	0.8410(4)	0.8418(3)
c (nm)	0.4746(4)	0.4752(3)
V (nm^3)	0.3357(6)	0.3367(5)
H_c (kOe)	3.32	4.35[a]

[a] randomly oriented powder.

uniaxially anisotropic 1:12 structure towards higher temperatures, simultaneously suppressing the 2:17R structure (which behaves as magnetically soft, even though it may also possess the uniaxial magnetic anisotropy due to the presence of Si [33]). It must be noted, however, that the outcome of the experiments described in this report must have been influenced not only be the thermodynamic equilibrium, by also by the rate of the reduction and the rate of the diffusion, both of which are likely to be specific for each of the components. Moreover, even the equilibrium R-Fe-Si phases in a finely structured system containing also CaO and Ca, may differ from those in the "bulk" R-Fe-Si alloys. It would be, therefore, premature to draw a general conclusion on the effect of the stabilizing effect of Zr on the 1:12 structure.

It is certain, however, that the Zr substitution for Sm significantly improves prospects of the products obtained under the described synthesis conditions as permanent magnet materials. If the $Sm_{0.7}Zr_{0.3}Fe_{10}Si_2$ powder had the $M(H)$ characteristic shown in Fig. 6 at its XRD density of 7.49 g/cm^3, the remanent magnetization and maximum energy product $(BH)_{max}$ would be 8.37 kG and 13.8 MGOe, respectively. The highest $(BH)_{max}$ reported to the date for the nanocrystalline $Sm(Fe,M)_{12}$ alloys is 8.4 MGOe [34]. The $Sm_{0.3}Ce_{0.3}Zr_{0.4}Fe_{10}Si_2$ powder (7.43 g/cm^3, 8.14 kG, 10.1 MGOe) containing *nominally* as little as 2.3 at% (6.1 wt%) Sm also compares favorably with these past data. Even though the nominal concentrations do not account for the significant excesses of the raw REs in the presented experiments, the used oxides are less expensive than the metallic REs, and the synthesis procedure is open for a further optimization. Among other characteristics the future optimization efforts should address is the less-than-perfect anisotropy of the powders; a larger fraction of single crystal particles must further increase the remanence and $(BH)_{max}$. It is also very important to find a method for compaction of the mechanochemically synthesized 1:12 powders into anisotropic fully dense magnets with appreciable properties.

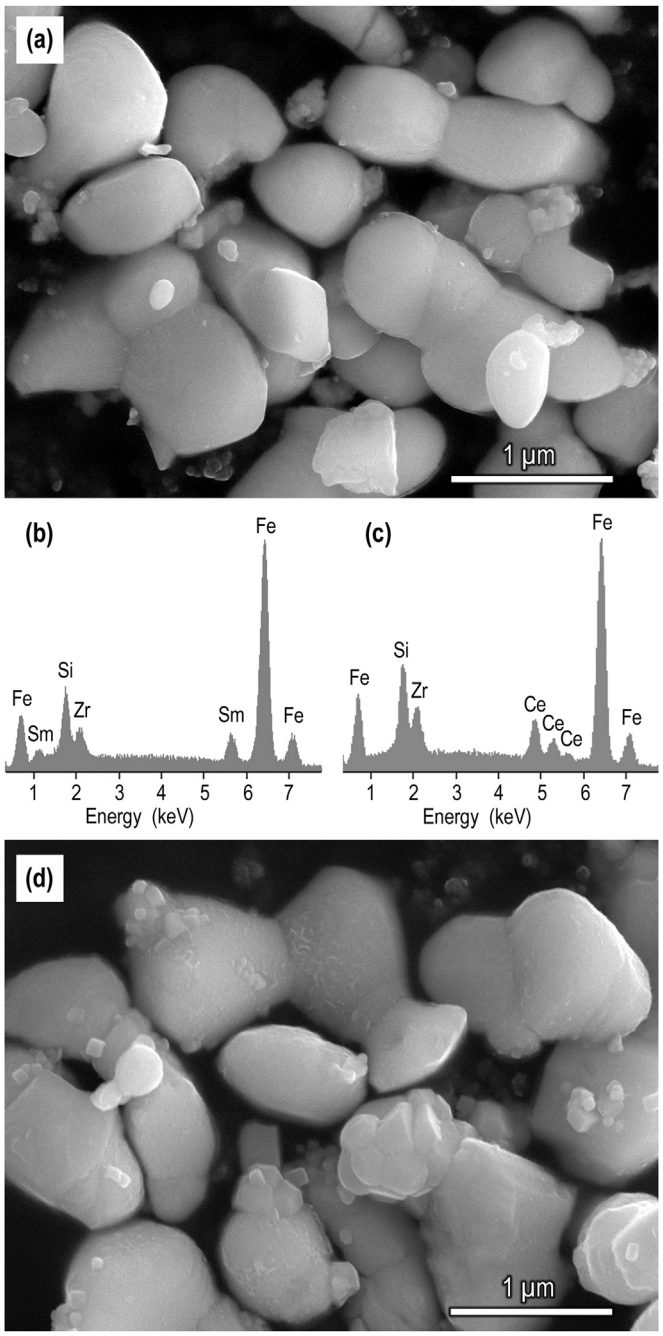

Fig. 5. SEM micrographs and EDS spectra of (a,b) $Sm_{0.7}Zr_{0.3}Fe_{10}Si_2$ and (c,d) $Ce_{0.6}Zr_{0.4}Fe_{10}Si_2$ powders collected (washed) after processing at $T_a = 1150$ °C.

5. Conclusion

The known advantages of the mechanochemistry – preparation of fine anisotropic particles with fewer defects and a higher H_c – are especially useful in the case of materials requiring high synthesis temperatures, such as the $RFe_{10}Si_2$. Under the used synthesis conditions, attaining of the 1:12 structure is strongly favored by 30–40% of the R element being represented by Zr. The resulting fine anisotropic powders feature both improved hard magnetic performance and lower nominal concentration of the rare earth, particularly Sm. Such powders may be of interest for the development of rare-earth-lean, Nd- and Co-free low-cost permanent magnets with the maximum energy product of 12–20 MGOe.

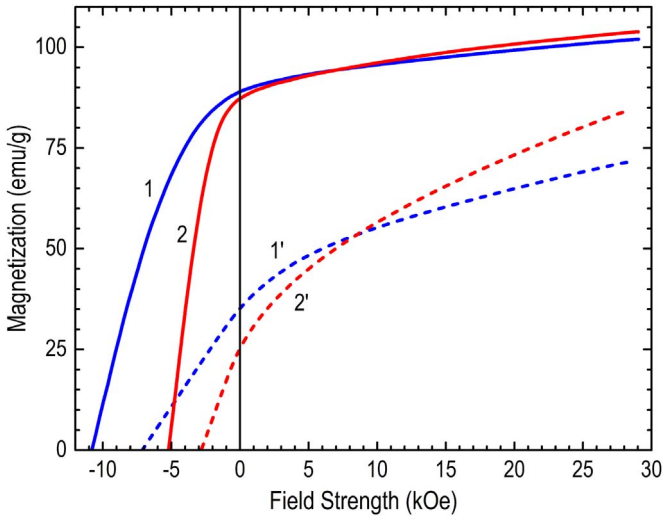

Fig. 6. Magnetization curves of powders collected (washed) after processing at $T_a = 1150$ °C and magnetically oriented: 1, 1′ – $Sm_{0.7}Zr_{0.3}Fe_{10}Si_2$; 2, 2′ – $Sm_{0.3}Ce_{0.3}Zr_{0.4}Fe_{10}Si_2$. The data are corrected for self-demagnetization.

Acknowledgments

This work was supported by Materials Sciences and Engineering Division of the US Department of Energy through a Basic Energy Sciences Program (Grant No. DE-FG02-04ER4612) and by University of Delaware Energy Institute.

References

[1] F. Ronning, S. Bader, Rare earth replacement magnets, J. Phys.: Condens. Matter 26 (2014) 1–3.
[2] T. Saito, H. Miyoshi, D. Nishio-Hamane, Magnetic properties of Sm–Fe–Ti nanocomposite magnets with a $ThMn_{12}$ structure, J. Alloy. Compd. 519 (2012) 144–148.
[3] S. Khazzan, L. Bessais, G. Van Tendeloo, N. Mliki, Correlation between the nanocrystalline $Sm(Fe,Mo)_{12}$ and its out of equilibrium phase $Sm(Fe,Mo)_{10}$, J. Magn. Magn. Mater. 363 (2014) 125–132.
[4] C. Zhou, M. Tessema, M.S. Meyer, F.E. Pinkerton, Synthesis of $CeFe_{10.5}Mo_{1.5}$ with $ThMn_{12}$-type structure by melt spinning, J. Magn. Magn. Mater. 336 (2013) 26–28.
[5] D. Goll, R. Loeffler, R. Stein, U. Pflanz, S. Goeb, R. Karimi, G. Schneider, Temperature dependent magnetic properties and application potential of intermetallic $Fe_{11-x}Co_xTiCe$, Phys. Status Solidi RRL 8 (2014) 862–865.
[6] C. Zhou, F.E. Pinkerton, J.F. Herbst, Magnetic properties of $CeFe_{11-x}Co_xTi$ with $ThMn_{12}$ structure, J. Appl. Phys. 115 (2014) 1–3.
[7] C. Zhou, D. Haddad, R.S. Kukreja, F.E. Pinkerton, K. Sun, M.J. Kramer, Magnetic hardening of $CeFe_{11}Ti$ and the effect of TiC addition, IEEE Trans. Magn. 52 (2015) 1–4.
[8] C. Zhou, F.E. Pinkerton, J.F. Herbst, High Curie temperature of Ce-Fe-Si compounds with $ThMn_{12}$ structure, Scr. Mater. 95 (2015) 66–69.
[9] C. Zhou, K. Sun, F.E. Pinkerton, M.J. Kramer, Magnetic hardening of $Ce_{11+x}Fe_{11-y}Co_yTi$ with $ThMn_{12}$ structure by melt spinning, J. Appl. Phys. 117 (2015) 1–4.
[10] S. Sakurada, A. Tsutai, M. Sahashi, A study on the formation of $ThMn_{12}$ and $NaZn_{13}$ structures in $RFe_{10}Si_2$, J. Alloy. Compd. 187 (1992) 67–71.
[11] A.M. Gabay, N.N. Shchegoleva, E.V. Belozerov, The structure and hard magnetic properties of rapidly quenched $(Sm,Zr)_1(Fe,Si)_{12}$ alloys, Phys. Met. Metallogr. 94 (2002) 252–257.
[12] A.M. Gabay, G.C. Hadjipanayis, $ThMn_{12}$-type structure and uniaxial magnetic anisotropy in $ZrFe_{10}Si_2$ and $Zr_{1-x}Ce_xFe_{10}Si_2$ alloys, J. Alloy. Compd. 657 (2016) 133–137.
[13] K.H.J. Bushow, Permanent magnet materials based on tetragonal rare earth compounds of the type $RFe_{12-x}M_x$, J. Magn. Magn. Mater. 100 (1991) 79–89.
[14] Y.Z. Wang, G.C. Hadjipanayis, Magnetic properties of Sm-Fe-Ti-V alloys, J. Magn. Magn. Mater. 87 (1990) 375–378.
[15] L. Schultz, K. Schnitzke, J. Wecker, High coercivity in mechanically alloyed Sm-Fe-V magnets with a $ThMn_{12}$ crystal structure, Appl. Phys. Lett. 56 (1990) 868–870.
[16] M. Okada, A. Kojima, K. Yamagishi, M. Homma, High coercivity in melt-spun $SmFe_{10}(Ti,M)_2$ ribbons (M=V/Cr/Mn/Mo), IEEE Trans. Magn. 26 (1990) 1376–1378.
[17] M. Solzi, R.H. Xue, L. Pareti, Magnetic anisotropy and first-order magnetization process in $Sm(Fe_{1-x}Co_x)_{10}M_2$ (M=Ti, Si) compounds, J. Magn. Magn. Mater. 88

(1996) 44–50.
[18] Q.F. Xiao, Z.D. Zhang, T. Zhao, W. Liu, Y.C. Sui, X.G. Zhao, D.Y. Geng, Crystallographic transformations of rapidly quenched $Sm_{10}Fe_{90-x}Ti_x$ and magnetic properties of their nitrides, J. Appl. Phys. 82 (1997) 6170–6176.
[19] J. Ding, M. Rosenberg, Magnetic properties of melt spun and crystallized $SmFe_{10}M_2$, J. Magn. Magn. Mater. 83 (1990) 257–258.
[20] A.M. Gabay, G.C. Hadjipanayis, Application of mechanochemical synthesis to manufacturing of permanent magnets, JOM 67 (2015) 1329–1335.
[21] A.M. Gabay, A. Martín-Cid, J.M. Barandiaran, D. Salazar, G.C. Hadjipanayis, Low-cost $Ce_{1-x}Sm_x(Fe,Co,Ti)_{12}$ alloys for permanent magnets, AIP Adv. 6 (2016) 1–6.
[22] M.Z. Su, S.F. Liu, X.L. Qian, J.H. Lin, An alternative approach to the finely crystalline powder of rare earth-transition metal alloys, J. Alloy. Compd. 249 (1997) 229–233.
[23] H. Saito, M. Takahashi, T. Wakiyama, Magnetic properties and structure change from tetragonal to hexagonal for the rapidly quenched $SmTiFe_{11}$ alloy ribbons, J. Appl. Phys. 64 (1988) 5965–5967.
[24] L. Bessais, C. Djega-Mariadassou, Structure and magnetic properties of nanocrystalline $Sm(Fe_{1-x}Co_x)_{11}Ti$ ($x \leq 2$), Phys. Rev. 63 (2001) 1–13.
[25] M. Katter, J. Wecker, L. Schultz, Structural and hard magnetic properties of rapidly solidified Sm-Fe-N, J. Appl. Phys. 70 (1991) 3188–3196.
[26] C. Djega-Mariadassou, L. Bessais, Emergence of order in nanocrystalline $SmFe_9$, J. Magn. Magn. Mater. 210 (2000) 81–87.
[27] G.V. Ivanova, G.M. Makarova, Ye.N. Shcherbakova, Ye.V. Belozerov, A. S. Yermolenko, Peculiarities of the $R_3(Fe,Si)_{29}$ phase formation in the Sm-Fe-Si system, J. Alloy. Compd. 260 (1997) 139–142.
[28] W. Kraus, G. Nolze, Powder cell – a program for the representation and manipulation of crystal structures and calculation of the resulting X-ray powder patterns, J. Appl. Crystallogr. 29 (1996) 301–303.
[29] K. Ohashi, Y. Tawara, R. Osugi, M. Shimao, Magnetic properties of Fe-rich rare-earth intermetallic compounds with a $ThMn_{12}$ structure, J. Appl. Phys. 64 (1988) 5714–5716.
[30] I. Felner, I. Mayer, A. Grill, M. Schieber, Magnetic ordering in rare earth iron silicides and germanides of the RFe_2X_2 type, Solid State Commun. 16 (1975) 1005–1009.
[31] E. Claude, S. Ram, I. Gimenez, P. Chaudoüet, D. Boursier, J.C. Joubert, Evidence of a quantitative relationship between the degree of hydrogen intercalation and the coercivity of the two permanent magnet alloys $Nd_2Fe_{14}B$ and $Nd_2Fe_{11}Co_3B$, IEEE Trans. Magn. 29 (1993) 2767–2769.
[32] F.E. Pinkerton, D.J. Van Wingerden, Magnetic hardening of $SmFe_{10}V_2$ by melt-spinning, IEEE Trans. Magn. 25 (1989) 3306–3308.
[33] W. Zarek, Influence of Si, A1 and C on the crystal structure and magnetic properties of Sm_2Fe_{17}, J. Magn. Magn. Mater. 157/158 (1996) 91–92.
[34] S. Sugimoto, A. Kojima, M. Okada, M. Homma, Enhancement of magnetic properties of $Sm(Fe,Co,Ti)_{12}$ melt-spun ribbons by refining crystallized grains, Mater. Trans. 32 (1991) 1180–1183.